

A Role for Histone H2B Variants in Endocrine-Resistant Breast Cancer

Shweta R Nayak¹ · Emily Harrington² · David Boone² · Ryan Hartmaier² · Jian Chen² ·
Thushangi N. Pathiraja³ · Kristine L. Cooper⁴ · Jeffrey L. Fine⁵ · Joseph Sanfilippo¹ ·
Nancy E. Davidson^{6,7} · Adrian V. Lee² · David Dabbs⁵ · Steffi Oesterreich²

Received: 27 March 2015 / Accepted: 9 June 2015 / Published online: 26 June 2015
© Springer Science+Business Media New York 2015

Abstract Acquired resistance to aromatase inhibitors (AIs) remains a major clinical problem in the treatment of estrogen receptor-positive (ER+) breast cancer. We and others have previously reported widespread changes in DNA methylation using breast cancer cell line models of endocrine resistance. Here, we show that the histone variant HIST1H2BE is hypomethylated in estrogen deprivation-resistant C4-12 and long-term estrogen-deprived (LTED) cells compared with parental MCF-7 cells. As expected, this hypomethylation associates with increased expression of HIST1H2BE in C4-12 and LTED cells. Both overexpression and downregulation of HIST1H2BE caused decreased proliferation in breast cancer

cell lines suggesting the need for tightly controlled expression of this histone variant. Gene expression analysis showed varied expression of HIST1H2BE in a large panel of breast cancer cell lines, without restriction to specific molecular subtypes. Analysis of HIST1H2BE messenger RNA (mRNA) expression in ER+ AI-treated breast tumors showed significantly higher expression in resistant ($n=19$) compared with sensitive ($n=37$) tumors ($p=0.01$). Using nanostring analysis, we measured expression of all 61 histone variants in endocrine-resistant and endocrine-sensitive tumors. We found significant overexpression of 22 variant histone genes in tumors resistant to AI therapy. In silico The Cancer Genome Atlas (TCGA) analysis showed frequent amplification of the HIST1 locus. In summary, our studies show, for the first time, that overexpression of histone variants might be important in endocrine response in ER+ breast cancer, and that overexpression is at least in part mediated via epigenetic mechanisms and amplifications. Future studies addressing endocrine response should include a potential role of these currently understudied histone variants.

Electronic supplementary material The online version of this article (doi:10.1007/s12672-015-0230-5) contains supplementary material, which is available to authorized users.

✉ Steffi Oesterreich
oesterreichs@upmc.edu

¹ Division of Reproductive Endocrinology, Magee-Womens Hospital, University of Pittsburgh Medical Center (UPMC), Pittsburgh, PA, USA

² Department of Pharmacology and Chemical Biology, Women's Cancer Research Center (WCRC), Magee-Womens Research Institute (MWRI), University of Pittsburgh Cancer Institute (UPCI), 204 Craft Avenue, Pittsburgh, PA 15213, USA

³ Genome Institute of Singapore, Singapore, Singapore

⁴ Biostatistics Core Facility at UPCI, Pittsburgh, PA, USA

⁵ Department of Pathology, Magee-Womens Hospital, UPMC, Pittsburgh, PA, USA

⁶ Department of Medicine, UPCI, UPMC, Pittsburgh, PA, USA

⁷ Department of Pharmacology and Chemical Biology, UPCI, UPMC, Pittsburgh, PA, USA

Introduction

The role of steroid hormone receptors in the proliferation of breast epithelial cells, along with their expression in cancer, makes them an attractive target for therapy. Nearly 70 % of breast tumors express ER, and thus are candidates for anti-estrogen therapy, including tamoxifen and aromatase inhibitors (AIs). However, if treated with tamoxifen, one third of women with ER-positive (ER+) disease will recur within 15 years [10]. Since completion of the Arimidex, Tamoxifen, Alone or in Combination (ATAC) trial, which revealed slightly superior efficacy of AI compared with tamoxifen, AIs have become the preferred first line therapy for postmenopausal

women with ER-positive disease [3]. As a considerable number of tumors still develop resistance, the understanding of the mechanisms of acquired endocrine resistance to AI is critical [1, 24].

Mechanisms of acquired resistance to AIs may include ligand-independent activation of estrogen signaling, alternative sources of estrogen, loss or mutation of ER, activation of growth factor receptors, and ineffective inhibition of aromatase [1, 11, 17, 24, 25]. There is also an increasing recognition of the role of epigenetics in tumorigenesis, including breast cancer [14]. For example, differential promoter methylation for a number of genes, including PTEN, PITX2, and CDK10, have been associated with resistance to tamoxifen but this has been less well studied in AI resistance [12, 15, 28]. There is currently no strong published evidence for regulation of enzymes controlling DNA methylation by estrogen signaling or hormone withdrawal.

We recently performed an unbiased study of genome-wide DNA methylation associated with resistance to estrogen deprivation, using C4-12 and long-term estrogen-deprived (LTED) cells [27]. These two cell lines are previously established MCF-7 subclones resistant to estrogen deprivation, are representative of clinical AI-resistant breast tumors [5, 16, 22, 23, 26, 33, 31, 32, 42]. Our previous studies had focused on hypermethylation of genes and here we set out to identify hypomethylated and overexpressed genes [27]. We identified hypomethylation of a number of histone variants, including the homomorphic variant HIST1H2BE. This variant is overexpressed in the resistant cell lines and in clinical specimens resistant to AI. While there are a number of reports on the role of H1 and H2A variants in normal physiology as well as in cancer [2, 36, 40], to our knowledge, this is the first report of a role for a H2B variant in breast cancer. In addition, we expanded the gene expression analysis to all histone variants and found significant associations between a number of variants and resistance to AI treatment, highlighting the need for further analysis of these relatively understudied genes.

Methods

Cell Culture

MCF-7 cell lines were obtained from the American Type Culture Collection (ATCC), and the C4-12 and LTED cell lines were generated and maintained as previously described [26, 32], and further outlined in the [Supplementary Methods](#). Breast cancer cell lines were obtained from the Integrative Cancer Biology Program (ICBP) 45 breast cancer cell line kit (ICBP45) of the National Cancer Institute. An RNA panel from normal tissue was purchased from Ambion/Life Technologies.

Patients and Tissue Samples

We obtained Institutional Review Board (IRB) approval to collect breast tumor specimens from the University of Pittsburgh Health Sciences Tumor Bank (HSTB). Our inclusion criteria included patients who (1) did not receive neoadjuvant chemotherapy (2) received AI therapy and (3) who were followed for at least 5 years. “Cases” were defined as tumors, which recurred less than 5 years ($n=17$), and “controls” were tumors, which did not recur for their period of documented follow-up ($n=37$). Clinical variables, including nodal status, tumor size, and site and time to recurrence were obtained for all tumors.

DNA Extraction, PCR, and Bisulfite Sequencing

Genomic DNA from the cell lines was isolated using the DNeasy blood and tissue kit (Qiagen) as recommended by the supplier. Genomic DNA was bisulfite converted using the EZ DNA methylation gold kit (Zymo Research) according to the supplier’s protocol and PCR amplified using Hotstar Taq Master Mix (Qiagen). After PCR amplification, the product was TA cloned using The Original TA Cloning Kit (Invitrogen), and DNA was isolated using the QIAprep Spin Miniprep Kit (Qiagen) and sequenced (GeneWiz, South Plainfield New Jersey). Bisulfite sequencing interrogated 2 CpG-rich regions for HIST1H2BE located at -184 and $+179$ from the transcription start site $+1$. We measured levels of DNA methylation as the percentage of bisulfite-resistant cytosines at CpG sites noted for HIST1H2BE for four clones. PCR and BS sequencing primer sequences along with annealing temperatures are listed in [Supplementary Tables 1 and 2](#) and cycling conditions described in the [Supplementary Methods](#).

RNA Extraction and Quantitative Real-Time PCR

RNA isolation for both cell lines and human frozen tissue samples was performed using the GE illustra RNAspin Mini Kit as recommended by the supplier. For frozen samples, tissues were first crushed under liquid nitrogen using a metal pestle and mortar. The messenger RNA (mRNA) expression was measured using quantitative real-time PCR (q-RT-PCR) assays using gene-specific primers (SYBR Green assay) by an ABI PRISM 7700 Sequence Detector (Applied Biosystems) and further outlined in the [Supplementary Methods](#). Relative fold change for each gene was calculated using the $\Delta\Delta C_t$ method as previously described [21], and the Student’s t test was used to determine statistical significance. Primers used for q-RT-PCR are listed in [Supplementary Table 3](#).

Protein Extraction and Immunoblot

Cells from in vitro culture were lysed with RIPA buffer and then sonicated briefly. Protein concentrations were determined by BCA assay and samples were boiled at 100 °C for 5 min mixed with loading buffer. Proteins were separated on SDS-PAGE gel and transferred to a polyvinylidene difluoride (PVDF) membrane. The PVDF membrane was blocked for 1.5 h at room temperature using Odyssey Blocking Buffer. Primary antibodies (anti-histone H2B antibody (ab18977, Abcam), beta-actin (Sigma A5441), tubulin (β tubulin, 2128S, Cell Signaling)) were incubated overnight at 4 °C and LI-COR® IRDye dye-conjugated secondary antibodies were incubated for 1 h at room temperature. Immunoreactive signals were detected by the Odyssey CLx Infrared Imaging system.

Generation of HIST1H2BE Stable Knockdown and Overexpressing Cell Lines

For the generation of stable HIST1H2BE knockdown cell lines, LTED cells were transduced with lentiviral particles containing small hairpin (RNA shRNA)mir-GFP to HIST1H2BE. The shuttle vectors for expression of shRNA were from Sigma. Gene-specific shRNA plasmids were co-transfected into 293-FT cells together with the packaging plasmids pMD2.g (VSVG), pRSV-REV, and pMDLg/pRRE. Forty-eight hours post-transfection, viral particles were collected in the culture supernatant, filtered (0.45 μ m), and either stored at –80 °C or used immediately to transduce the target cells. Scrambled (SCR) shRNA was transduced as a control. Target sequences are listed in Supplementary Table 4 for knockdown clones, sh1, sh2, and sh3. Stably integrated cells were selected by adding 1 μ g/mL puromycin (Invitrogen) to the culture medium for 4 weeks. For overexpression, HIST1H2BE cDNA was ligated into a PEF-1/myc-His A vector (Invitrogen). Forward and Reverse target sequences are shown in Supplementary Table 4 and contained *Not1* and *BamH1* restriction sites respectively. MCF-7 cells were transfected using FuGene6 transfection reagent (Roche) and stably integrated cells were selected by adding Geneticin 50 μ g/mL (Invitrogen).

Analysis of Cellular Phenotypes

Details of plating conditions and determination of standard growth curves are outlined in the [Supplementary Methods](#). For growth curves, plates were analyzed for cell count daily for a duration of five days using FluoReporter® Blue Fluorometric dsDNA Quantitation Kit (Invitrogen) according to the manufacturer's protocol. Fluorescence was then immediately read using a VICTOR™ X4 Multilabel plate reader at an excitation of 360 nm and emission of 460 nm (Perkin Elmer).

Nanostring Analysis

For the nCounter Gene Expression assay, probes were hybridized to 100 ng of total RNA for 18 h at 65 °C and applied to the nCounter™ Preparation Station for automated removal of excess probe and immobilization of probe-transcript complexes on a streptavidin-coated cartridge. Data were collected using the nCounter™ Digital Analyzer by counting the individual barcodes. All counts were normalized to the internal housekeeping genes and to positive and negative controls in each hybridization reaction. Probe sequences are listed in Supplementary Table 5.

Statistical Analysis

Unless otherwise indicated, “asterisk” in figures refers to $p < 0.05$. Two-sample *t* tests were used for two group comparisons, and one-way ANOVA along with Tukey's post-test was used for multiple group comparisons. For growth curves, data was first log transformed and compared by linear regression for differences in slopes. For analysis of tumor samples, the mean of the *RPS11* Ct measurements was subtracted from the mean of the HIST1H2BE Ct measurements to obtain the Δ Ct value. The Wilcoxon rank-sum test was used to test the null hypothesis that the distribution of the Δ Ct values for the controls and the cases is the same. For nanostring analysis, raw mRNA counts from the nCounter platform were normalized first to the geometric mean of onboard-positive controls followed by normalization to the geometric mean of the housekeeping genes to adjust for sample content. Statistical methods were applied to the log-transformed data and comparisons between cases and controls were made using the two-sample *t* test controlling the false discovery rate at 5 %. Statistical analysis was performed using R version 2.15.2 (2012) and the normalization of nCounter data was performed with R package NanoStringNorm [41].

Results and Discussion

Hypomethylation and Overexpression of HIST1H2BE in Cell Line Models of AI Resistance

We previously reported a genome-wide methylation screen in the endocrine-resistant cell lines C4-12 and LTED that revealed many differentially methylated genes [27]. This screen used affinity-based enrichment of methylated regions of DNA via a methylation-binding domain (MBD). While our previous studies focused on genes hypermethylated in C4-12 and LTED, here we set out to identify hypomethylated and overexpressed genes. Using a fold change cutoff > 2 , 82, and 97 hypomethylated genes were identified in C4-12 and LTED, respectively. Among the 15 genes that were differentially

hypomethylated in both cell lines (Supplementary Table S6), there were two histone variant genes. Further analysis of the MBD pull-down array data showed differential methylation of a number of variants of the four core histone proteins H2A, H2B, H3, and H4, as well as the linker histone H1 (Supplementary Table S7). These histone variants are thought to provide alternative mechanisms for introducing variations into the eukaryotic epigenome, for example, by regulation of temporal and tissue-specific gene expression (for recent reviews, see [2, 36, 40]). H2A variants are generally the most diverse family of the core proteins, with well-described roles for H2A.X, H2A.Z, and MacroH2A [23, 30–37]. Homomorphous variants are located within the histone loci, are expressed in a replication-dependent manner, and have minor sequence changes compared to the canonical proteins. In contrast, heteromorphous variants are located outside the histone loci, are expressed in replication-independent manners, and have major sequence changes compared to the canonical proteins.

We observed altered methylation at HIST1H1A, HIST1H2BB, HIST1H2BE, HIST1H3A, HIST1H3C, HIST1H4D, and HIST1H4F. Visual inspection of methylation

array data showed consistent hypomethylated peaks for HIST1H2BE, HIST1H3A, HIST1H3C, and HIST1H4D in both C4-12 and LTED cell compared with MCF-7 cells (Supplementary Table S7). Expression analysis of these four genes using q-RT-PCR revealed overexpression of HIST1H3A, HIST1H3C, and HIST1H2BE in the resistant cell lines, with the latter showing strongest overexpression in both models (Fig. 1a). Of note, short-term deprivation of MCF-7 cells of estrogen (1–24 h) did not result in an increase in HIST1H2BE expression (data not shown).

HIST1H2BE is one of five homomorphous variants (HIST1H2BC, HIST1H2BE, HIST1H2BF, HIST1H2BG, and HIST1H2BI) of the canonical histone H2B. The five proteins are coded for by five unique single exon-genes at the HIST1 locus on chromosome 6p21-22 (Supplementary Fig. S1a), that differ at the genomic level sufficiently to generate variant-specific primers, however, the five proteins are identical in their amino acid sequence (Supplementary Fig. S1b). Potential unique roles for these variants have not been studied to our knowledge, as we were unable to find any publications on the roles of the HIST1H2BC/E/F/G/I

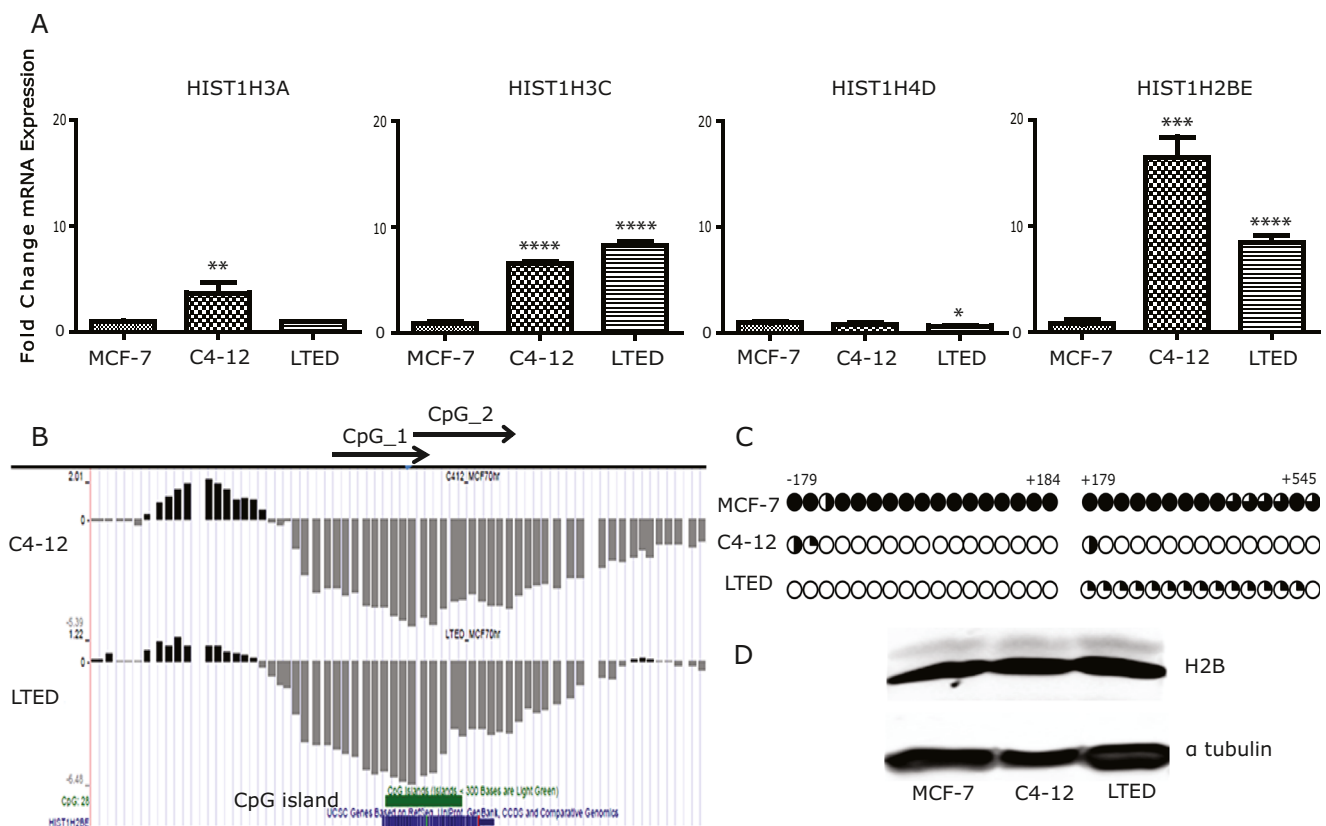


Fig. 1 Hypomethylation and overexpression of HIST1H2BE in endocrine-resistant cell breast cancer cells. **a** Relative mRNA expression of histone variants HIST1H3A, HIST1H3C, HIST1H4B, and HIST2BE was measured by RT-qPCR in C4-12, LTED, and MCF-7 cells and analyzed by Student's *t* test. **** $p < 0.0001$. **b** Results of MBD-PD mapped to the University of California Santa Cruz (UCSC) Genome Browser (hg18). Hypermethylated and hypomethylated regions in C4-12 and LTED relative

to MCF-7 are represented by *upward black and downward gray bars*, respectively. Locations of HIST1H2BE and CpG island are indicated on the bottom. **c** Results of the bisulfite sequencing assay for HIST1H2BE MCF-7, C4-12, and LTED. Each CpG site is represented by a *circle*, and the percent of methylation at each site is shown by the *fraction of black shading*. **d** Immunoblot using antibody against H2B and Tubulin was used as loading control

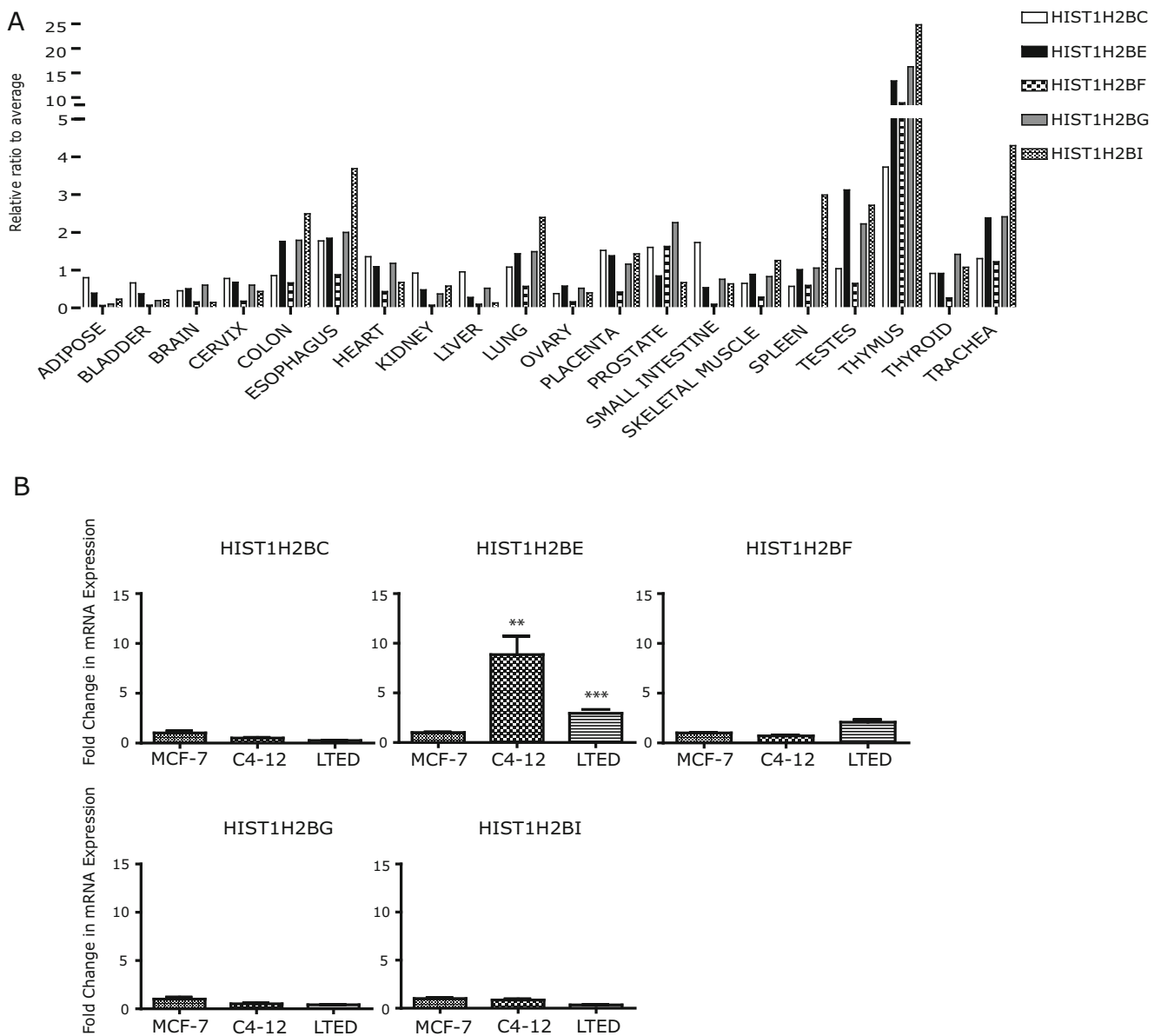


Fig. 2 HIST1H2BE is a unique homomorphous variant of H2B. **a** Relative mRNA expression of HIST1H2BC/E/F/G/I variants in a panel of normal tissue, expressed as fold change compared with the average of all variants

within a particular tissue. **b** Relative mRNA expression of H2B variants in MCF-7, C4-12, and LTED measured by q-RT-PCR. Student's *t* test was used for analysis (** $p < 0.001$)

proteins. An additional H2BE variant, HIST2H2BE, showing a change at a single amino acid (V40I) (Supplementary Fig. S1c), maps to the HIST2 locus on chromosome 1q21.2, and was reported to be functionally expressed in olfactory chemosensory neurons [34]. Notably, despite only a single amino acid difference, there is great variation at the genomic level when the coding region is compared with that of the homomorphous variant HIST1H2BE at the genomic level (Supplementary Fig. S1d).

The hypomethylation of HIST1H2BE in C4-12 and LTED overlaps with a CpG island in the exonic region of HIST1H2BE (Fig. 1b). Bisulfite sequencing of regions -179

to +184 bp, and +179 bp to +545 bp confirmed methylation in MCF-7 cells, and complete lack of methylation in both C4-12 and LTED cells (Fig. 1c). The mRNA overexpression of the variant was not sufficient to observe overexpression at the total H2B protein level, using a pan-H2B antibody (Fig. 1d). This was not surprising since variant proteins usually only represent small portions of the total cellular histone pool [2, 36]. Collectively, these data show that the homomorphous HIST1H2BE variant is overexpressed in two independent cell line models of AI resistance compared with their parental hormone-responsive MCF-7 line, likely as a result of epigenetic changes involving DNA hypomethylation.

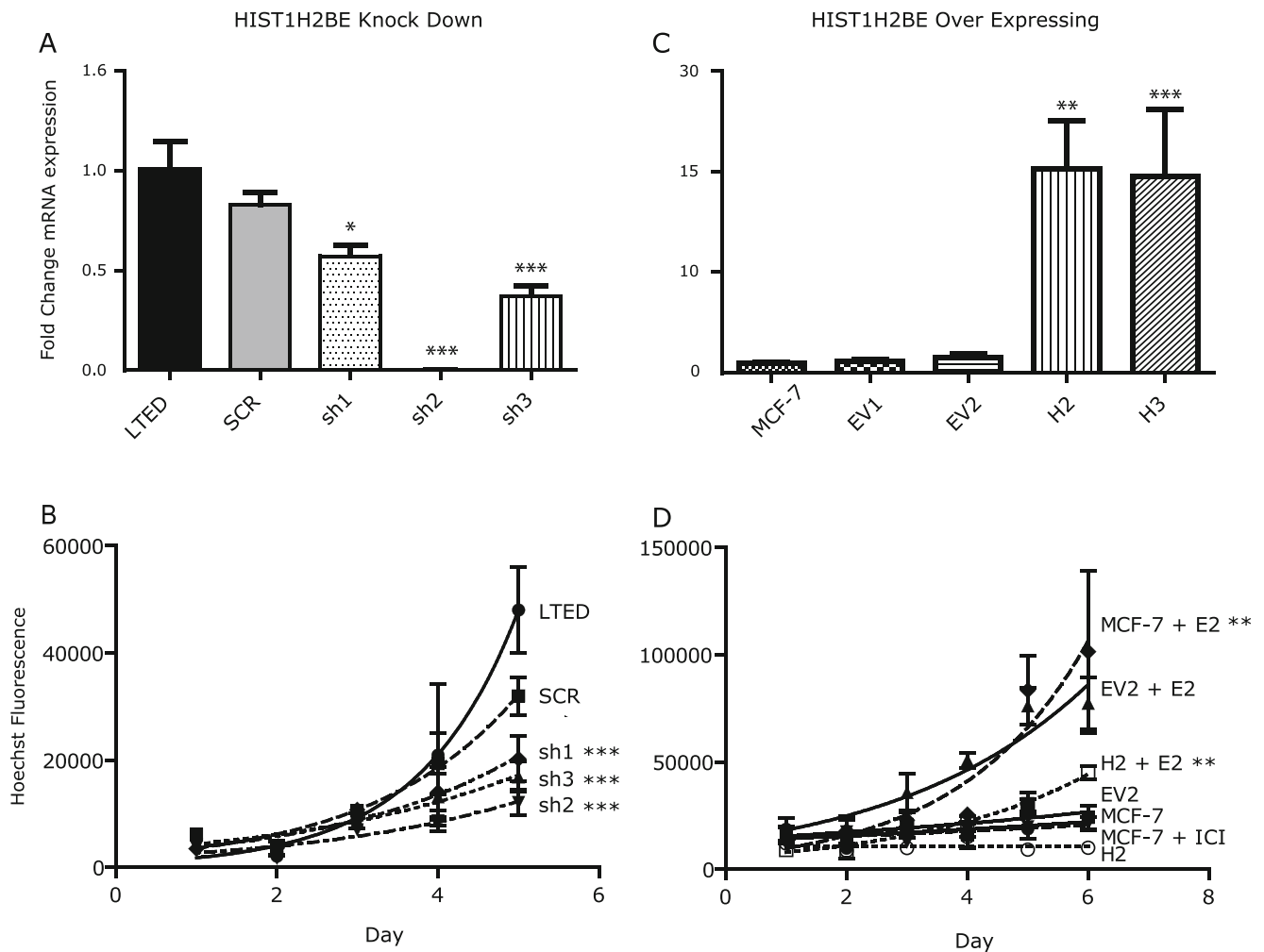


Fig. 3 HIST1H2BE knockdown and overexpression affect growth of breast cancer cells. **a** Relative mRNA expression of HIST1H2BE knockdown clones (sh1, sh2, sh3) compared with non-infected cells (LTED), and cells infected with scrambled control virus (SCR). Expression was analyzed using one-way ANOVA followed by Tukey's post-test for multiple comparison (** $p < 0.001$). **b** Growth curves for control cells and cells with HIST1H2BE knockdown. Values represent means \pm SEM of 2 experiments performed in technical triplicate. Growth was analyzed

using non-linear regression and an exponential growth equation (** $p < 0.001$). **c** Relative mRNA expression of HIST1H2BE overexpressing clones (H2, H3) compared with non-transfected MCF-7 cells and cells transfected with vector only (–EV1 and –EV2). Measurement was performed as described in (a). **d** Growth of overexpressing cells (H2) compared with control cells. Cells were kept in 5% CSS for 3 days before treatment with 10^{-9} M estradiol. Measurement was performed as described in (b) (** $p < 0.05$)

Expression and Sequence Analysis of HIST1H2BC/E/F/G/I Variants in MCF-7 and Resistant Clones

Given the paucity of information on the HIST1H2BE and its highly related C/E/F/I variants, we first measured their mRNA expression in a panel of normal tissues. Diversity at the nucleotide level allowed for generation of variant-specific primers (Supplementary Tables S1–S3). HIST1H2BE was highly expressed in testes and thymus and was expressed at low levels in liver, similar to most other H2B variants (Fig. 2a). In most tissues, with the exception of ovary and testes, HIST1H2BE was not the leading contributor of the five variants coding for a protein

with an identical amino acid sequence (Fig. 2a), however, in general there was good concordance in the tissue-specific expression of the five variants.

We next asked the question of whether overexpression in C4-12 and LTED was unique for HIST1H2BE. Expression analysis using RNA from the MCF-7, C4-12, and LTED cells revealed that significant overexpression in both resistant lines was only seen for HIST1H2BE and not for H2BC/F/G/I (Fig. 2b). HIST1H2BF was moderately yet not significantly overexpressed in LTED cells.

The unique epigenetic and expression changes of H2BE in these models of resistance were surprising given the identical protein sequence of the five variants. Given the recent

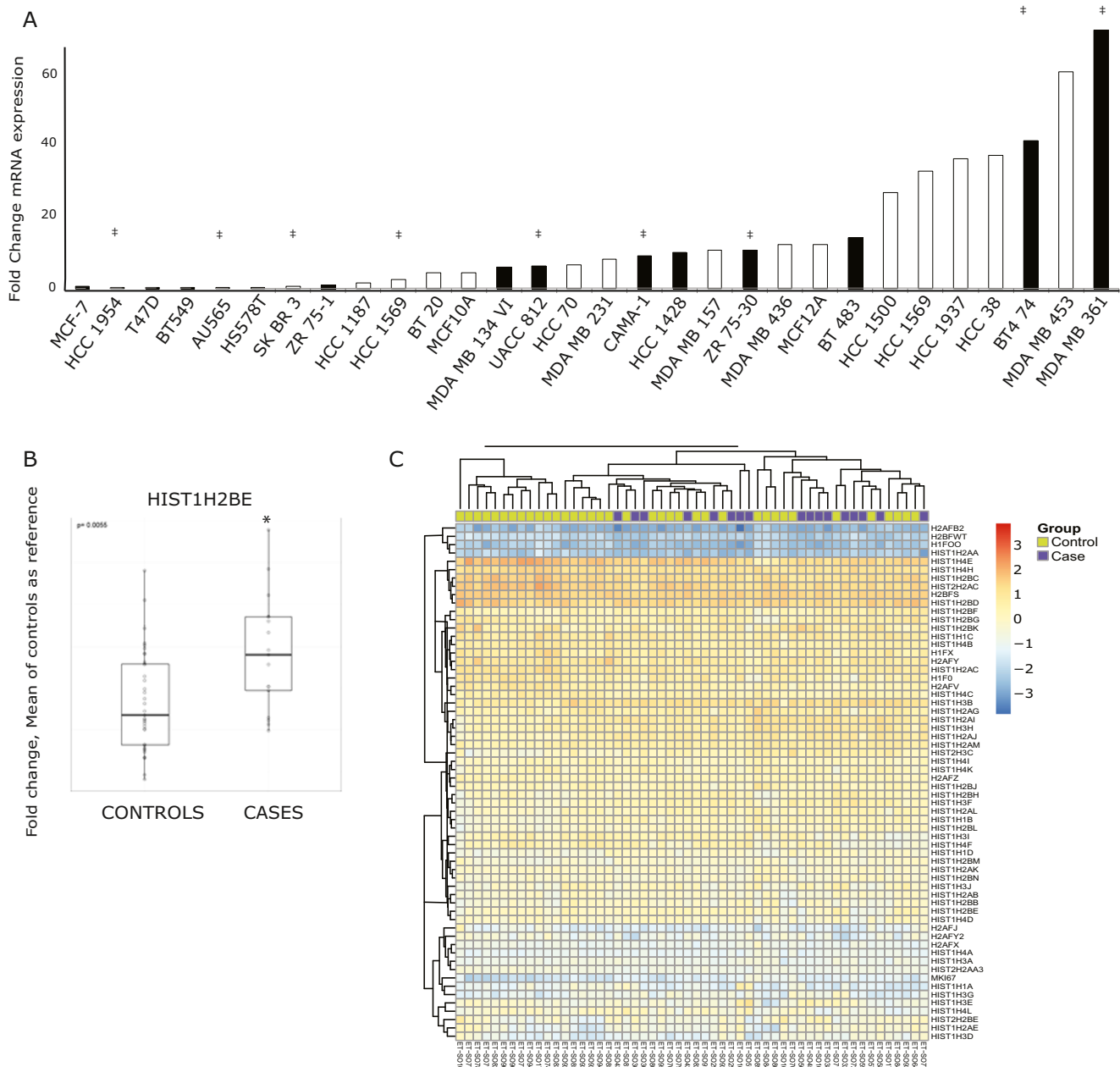


Fig. 4 HIST1H2BE, and other histone variants, are overexpressed in endocrine-resistant breast tumors. **a** Relative mRNA expression of HIST1H2BE in a panel of breast cancer cell lines, presented as fold change compared with MCF-7, measured by q-RT-PCR. ER+ and ER- cell lines shown in *black and white bars*, respectively, and Her2 overexpression is indicated with †. **b** Relative mRNA expression of HIST1H2BE in endocrine-sensitive and endocrine-resistant tumors,

measured by q-RT-PCR. *RPS11* was used as control, and primer sequences are shown in the [Electronic Supplementary Material](#). *Boxplots* represent the median, 25th, and 75th percentiles of fold change in expression, with the *whiskers* extending to 1.5 times the range between the 25th and 75th percentiles ($p=0.055$). **c** Heat map of histone variants expression ($n=61$) and Ki67 by nanostring analysis in tumors from cases and controls

identification of mutations in histone variants in gliomas, head and neck squamous cell carcinoma, and endometrial cancer [18], we reasoned that the variant genes might be mutated. Sequencing of the complete coding regions of the five homomorphic H2B variants in all three cell lines failed to reveal any mutations. We also tested whether the variants are expressed during different phases of the cell cycle to possibly identify unique roles but were unable

to find any evidence for such differential expression (data not shown). Future studies will include the analysis of unique posttranslational modifications and/or subcellular localization or even potential roles of the RNA. Thus, we observed unique overexpression of the homomorphic histone variant HIST1H2BE in two cell line models of AI resistance that was not associated with the development of variant-specific mutations.

Table 1 Patient and tumor characteristics. RNA was isolated from AI-treated ER+ tumors from patients who had not recurred (“AI-sensitive,” “controls,” $n=37$) or who recurred within 5 years after diagnosis (“resistant,” “cases,” $n=17$)

	AI sensitive (controls; $N=37$)	AI resistant (cases; $N=17$)	Fisher's exact test of t test p value
Age at diagnosis (years) mean (SD) [min, max]	62 (10) [44,81]	60 (12) [35,78]	0.4533
Date diagnosis	2002–2005	2002–2006	NA
Disease-free follow-up (years) median [min, max]	8.6 [5.0, 11.9]	3.3 [1.9, 4.6]	NA
Histology			
IDC	24 (65 %)	13 (76 %)	0.7352
ILC, mixed, or other	5 (14 %)	1 (6 %)	
Tumor size	8 (22 %)	3 (18 %)	
Stage			
1	17 (46 %)	6 (35 %)	0.5414
2	16 (43 %)	8 (47 %)	
3	4 (11 %)	2 (12 %)	
4	0 (0 %)	1 (6 %)	
PR+	31 (84 %)	13 (76 %)	0.7075
Adjuvant chemotherapy	18 (49 %)	7 (41 %)	0.7703
Radiation therapy	21 (57 %)	15 (88 %)	0.0303
Grade			
1	13 (36 %)	0 (0 %)	0.0024
2	17 (47 %)	8 (50 %)	
3	6 (17 %)	8 (50 %)	

Tumors from patients treated with neoadjuvant therapy were excluded

Altered H2BE Expression Inhibits Growth of Breast Cancer Cells

In order to determine whether overexpression of HIST1H2BE confers growth advantage to the LTED cells, we lowered HIST1H2BE levels using lentiviral infection of shRNA plasmids. We generated stable clones showing mRNA levels decreased by 40–90 % (Fig. 3a), and as expected, protein levels of total HIST1H2B were not altered (Supplementary Fig. S2a). LTED cells were generated in CSS and are continuously grown under these conditions. We observed significantly slower growth of LTED cells (Fig. 3b), suggesting that HIST1H2BE is necessary for full proliferation. In order to test whether this is unique for HIST1H2BE, we also lowered expression of HIST1H2BF, an H2B variant that showed a trend for higher expression in LTED cells (Fig. 2b). Downregulation of HIST1H2BF by 80 % did not result in any significant effect on growth (data not shown).

To study the potential role of HIST1H2BE overexpression in MCF-7 cells, we generated stable overexpressing clones. These clones showed 10- to 13-fold increased RNA expression (Fig. 3c). Protein overexpression was confirmed by immunoblotting with a myc-antibody (Supplementary Fig. S2b). While there was no significant difference between control and overexpressing cells in 10 % FBS (data not shown), the HIST1H2BE overexpressing cells showed decreased response

to estrogen stimulation (results for clones H2 and H3 are shown in Fig. 3d and Supplementary Fig. 2c, respectively). This was not a result of altered ER protein expression as measured by quantification of immunoblots (data not shown and Supplementary Fig. S2d). We also observed significantly increased anchorage-independent growth of stable overexpressing clone H2; however, this was not seen in the other clone (Supplementary Fig. S2e).

In summary, these data suggest that HIST1H2BE levels are critical for cell growth and estrogen response in breast cancer cells. Future studies need to address details of its function, including its genome-wide incorporation into chromatin, with a special focus on estrogen-regulated genes.

Overexpression of Histone Variants in Tumors Resistant to AI Treatment

Overexpression of CENP-A (a Histone H3-like centromeric protein A), H2A.Z, and other histone variants been described in a number of tumors, and H2A.Z has been suggested to contribute to endocrine resistance and was recently proposed as a potential therapeutic target in breast cancer [4, 7–9, 13, 19, 20, 29, 35, 38, 39].

To better understand a potential role of HIST1H2BE in breast cancer, we used RT-qPCR to characterize its expression in a panel of normal-like breast cells and breast cancer cell lines, representing various luminal and basal molecular

subtypes of breast cancer. Dynamic HIST1H2BE expression was seen across all cell lines, without restriction to specific subtypes (Fig. 4a). Next, we asked the question whether HIST1H2BE was differentially expressed in endocrine-sensitive and endocrine-resistant tumors. We isolated RNA from 56 ER+ tumors from patients treated with AI who either recurred within 5 years after diagnosis (resistant “cases,” $n=19$) or who had not recurred (sensitive “controls,” $n=37$). The detailed description of the clinical and pathological data for the patients in this cohort is shown in Table 1. The dates of diagnoses were between 2002 and 2005 (controls) or 2006 (cases), and the median disease-free follow-up for controls and cases are 8.6 and 3.3 years, respectively. There is a balanced distribution of most patient and tumor characteristics, except that the AI-resistant tumors had more high-grade tumors ($p=0.0024$). We measured HIST1H2BE by RT-qPCR and found significantly increased HIST1H2BE expression in resistant disease, i.e., in AI-treated tumors that recurred within 5 years ($p=0.01$) (Fig. 4b), consistent with the overexpression seen in our *in vitro* models.

Given the paucity of data on the role of histone variants in endocrine response, we set out to measure expression of all histone variants in the same tumor cohort of AI-treated tumors. Therefore, we generated a nanostring library probing expression of 61 histone variants. Unsupervised analysis of the expression profiles showed wide expression ranges of the histones (Fig. 4c) with the highest expression seen for HIST1H4E, HIST1H4H, HIST1H2BC, HIST2H2AC, H2BFS, and HIST1H2BD. Four histones, H2AFB2, HSBFWT, H1FOO, and HIST1H2AA were not expressed in breast cancer, which was expected for the testis- and oocyte-specific variants HSBFWT and H1FOO [6, 37]. The proliferation marker Ki67, which was included as a control, was expressed significantly higher in the primary tumors that recurred early, as expected ($p=0.0037$). Intriguingly, 22 histone variants were significantly overexpressed in recurrent tumors compared with controls (Table 2) (Supplementary Fig. S3a). Among those variants, 21 mapped to the HIST1 locus on 6p21-22 and one mapped to the HIST2 locus on 1q21 (Supplementary Fig. S3b). There was a trend for higher expression of HIST1H2BE in the AI-resistant tumors; however, in contrast to the RT-qPCR analysis, this did not reach significance in the nanostring analysis. The reason could include some inaccuracy of PCR due to amplification step, problems with the HIST1H2BE nanostring probe, or a relatively small effect that loses significance when many genes are measured and correction of multiple comparisons is applied. Importantly, the trend is the same for HIST1H2BE with higher expression in the resistant tumors, and in addition, we discovered that a large number of histone genes are overexpressed in AI-resistant breast tumors, suggesting that this family of proteins plays an important role in the development of endocrine-resistant breast cancer. Our analysis of The Cancer Genome

Table 2 Histone variants overexpressed in AI-resistant disease

Gene	<i>Q</i> value
HIST1H1B	0.0072
HIST1H1D	0.0011
HIST1H2AE	3.00E-04
HIST1H2AI	0.0054
HIST1H2AJ	0.0039
HIST1H2AL	0.0096
HIST1H2AM	0.0186
HIST1H2BB	0.048
HIST1H2BF	0.0051
HIST1H2BG	0.0299
HIST1H2BH	4.00E-04
HIST1H2BK	0.0229
HIST1H2BL	0.048
HIST1H2BM	0.0299
HIST1H3B	0.0347
HIST1H3D	0.0039
HIST1H3E	0.0096
HIST1H3F	2.00E-04
HIST1H3G	0.0146
HIST1H3H	0.0148
HIST1H4K	0.0238
HIST2H3C	0.0096

Raw values from nCounter platform were normalized to the geometric mean of positive controls followed by normalization to the geometric mean of the housekeeping genes to adjust for sample content. Statistical methods were applied to the log-transformed data and comparisons between cases and controls were made using the two-sample *t* test controlling the false-discovery rate at 5 %

Atlas (TCGA) data lends further support for a critical role of many of the variants, since many of them were frequently amplified (>5–10 % of samples) in primary breast cancer. When we examined all TCGA identified mutations across all histone variants, one mutation (HIST1H2BC E114K) was also found in a breast cancer metastasis [30]. Interestingly, we did not observe increased but decreased HIST1H2BE expression in tamoxifen-resistant MCF-7 subclones (data not shown), suggesting differential roles in AI and tamoxifen resistance. Clearly, further studies are needed to fully interrogate the impact of alterations in histone variant genes on breast cancer onset and metastasis.

In summary, our studies provide evidence that histone variants might be important players in the development of endocrine resistance in breast cancer. Specifically, we show a potential role for the H2B family of variants, which have previously been unrecognized compared with H2A variants.

Acknowledgments We would like to thank the Reproductive Endocrinology and Infertility fellowship program at the Magee-Womens Hospital of UPMC and specifically Drs. Anthony N Wakim, Tony Plant, and Kyle Orwig, who provided critical support throughout the studies. We would also like to thank Dr. Richard Santen at University of Virginia Health Sciences Center, Charlottesville, VA, for providing LTED cells, Dr. Gannon, whose group was instrumental in the generation of original screening data previously published (27), and Dr. Danny Hochbaum for outstanding guidance for cloning approaches. This project was in part funded through an Alexander von Humboldt Foundation fellowship (SO), a DOD predoctoral fellowship DOD 5W81XWH-06-1-0713 (T.N. Pathiraja), R01CA097213 (SO), Breast Cancer Research Foundation (ND, AVL, and SO), John Lazo Fellowship from the Department of Pharmacology (EAH), and a grant from the Pennsylvania Department of Health (SO, AVL). The Department specifically disclaims responsibility for any analyses, interpretations or conclusions. Lentivirus particles were provided by UPCI Core Facility, supported by Cancer Center Support grant NIH 5P30 CA47904.

Conflict of Interest The authors declare that they have no conflict of interest.

References

- Anderson H, Bulun S, Smith I, Dowsett M (2007) Predictors of response to aromatase inhibitors. *J Steroid Biochem Mol Biol* 106(1–5):49–54. doi:10.1016/j.jsbmb.2007.05.024
- Ausio J (2006) Histone variants—the structure behind the function. *Brief Funct Genomic Proteomic* 5(3):228–243. doi:10.1093/bfgp/ell020
- Baum M (2002) The ATAC (arimidex, tamoxifen, alone or in combination) adjuvant breast cancer trial in postmenopausal patients: factors influencing the success of patient recruitment. *Eur J Cancer* 38(15):1984–1986
- Biermann K, Heukamp LC, Steger K, Zhou H, Franke FE, Guetgemann I, Sonnack V et al (2007) Gene expression profiling identifies new biological markers of neoplastic germ cells. *Anticancer Res* 27(5A):3091–3100
- Chan CM, Martin LA, Johnston SR, Ali S, Dowsett M (2002) Molecular changes associated with the acquisition of oestrogen hypersensitivity in MCF-7 breast cancer cells on long-term oestrogen deprivation. *J Steroid Biochem Mol Biol* 81(4–5):333–341
- Churikov D, Siino J, Svetlova M, Zhang K, Gineitis A, Morton Bradbury E, Zalensky A (2004) Novel human testis-specific histone H2B encoded by the interrupted gene on the X chromosome. *Genomics* 84(4):745–756. doi:10.1016/j.ygeno.2004.06.001
- Conerly ML, Teves SS, Diolaiti D, Ulrich M, Eisenman RN, Henikoff S (2010) Changes in H2A.Z occupancy and DNA methylation during B-cell lymphomagenesis. *Genome Res* 20(10):1383–1390. doi:10.1101/gr.106542.110
- Dryhurst D, McMullen B, Fazli L, Rennie PS, Ausio J (2012) Histone H2A.Z prepares the prostate specific antigen (PSA) gene for androgen receptor-mediated transcription and is upregulated in a model of prostate cancer progression. *Cancer Lett* 315(1):38–47. doi:10.1016/j.canlet.2011.10.003
- Duncan DS, McWilliam P, Tighe O, Parle-McDermott A, Croke DT (2002) Gene expression differences between the microsatellite instability (MIN) and chromosomal instability (CIN) phenotypes in colorectal cancer revealed by high-density cDNA array hybridization. *Oncogene* 21(20):3253–3257. doi:10.1038/sj.onc.1205431
- Early Breast Cancer Trialists' Collaborative, Group (2005) Effects of chemotherapy and hormonal therapy for early breast cancer on recurrence and 15-year survival: an overview of the randomised trials. *Lancet* 365(9472):1687–1717. doi:10.1016/S0140-6736(05)66544-0
- Fuqua SA, Gu G, Rechoum Y (2014) Estrogen receptor (ER) alpha mutations in breast cancer: hidden in plain sight. *Breast Cancer Res Treat* 144(1):11–19. doi:10.1007/s10549-014-2847-4
- Harbeck N, Nimmrich I, Hartmann A, Ross JS, Cufer T, Grutzmann R, Kristiansen G et al (2008) Multicenter study using paraffin-embedded tumor tissue testing PITX2 DNA methylation as a marker for outcome prediction in tamoxifen-treated, node-negative breast cancer patients. *J Clin Oncol* 26(31):5036–5042. doi:10.1200/JCO.2007.14.1697
- Hua S, CB Kallen, R Dhar, MT Baquero, CE Mason, BA Russell, PK Shah et al. (2008) Genomic analysis of estrogen cascade reveals histone variant H2A.Z associated with breast cancer progression. *Mol Syst Biol* 4:188. doi:10.1038/msb.2008.25
- Huang Y, Nayak S, Jankowitz R, Davidson NE, Oesterreich S (2011) Epigenetics in breast cancer: what's new? *Breast Cancer Res* 13(6):225. doi:10.1186/bcr2925
- Iorns E, Turner NC, Elliott R, Syed N, Garrone O, Gasco M, Tutt AN, Crook T, Lord CJ, Ashworth A (2008) Identification of CDK10 as an important determinant of resistance to endocrine therapy for breast cancer. *Cancer Cell* 13(2):91–104. doi:10.1016/j.ccr.2008.01.001
- Jeng MH, Shupnik MA, Bender TP, Westin EH, Bandyopadhyay D, Kumar R, Masamura S, Santen RJ (1998) Estrogen receptor expression and function in long-term estrogen-deprived human breast cancer cells. *Endocrinology* 139(10):4164–4174. doi:10.1210/endo.139.10.6229
- Johnston SR, Dowsett M (2003) Aromatase inhibitors for breast cancer: lessons from the laboratory. *Nat Rev Cancer* 3(11):821–831. doi:10.1038/nrc1211
- Kandoth C, McLellan MD, Vandin F, Ye K, Niu B, Lu C, Xie M et al (2013) Mutational landscape and significance across 12 major cancer types. *Nature* 502(7471):333–339. doi:10.1038/nature12634
- Kapoor A, Goldberg MS, Cumberland LK, Ratnakumar K, Segura MF, Emanuel PO, Menendez S et al (2010) The histone variant macroH2A suppresses melanoma progression through regulation of CDK8. *Nature* 468(7327):1105–1109. doi:10.1038/nature09590
- Li YM, Liu XH, Cao XZ, Wang L, Zhu MH (2007) Expression of centromere protein a in hepatocellular carcinoma. *Zhonghua Bing Li Xue Za Zhi* 36(3):175–178
- Livak KJ, Schmittgen TD (2001) Analysis of relative gene expression data using real-time quantitative PCR and the 2^{-ΔΔC_t} method. *Methods* 25(4):402–408. doi:10.1006/meth.2001.1262
- Martin LA, Pancholi S, Chan CM, Farmer I, Kimberley C, Dowsett M, Johnston SR (2005) The anti-oestrogen ICI 182,780, but not tamoxifen, inhibits the growth of MCF-7 breast cancer cells refractory to long-term oestrogen deprivation through down-regulation of oestrogen receptor and IGF signalling. *Endocr Relat Cancer* 12(4):1017–1036. doi:10.1677/erc.1.00905
- Masamura S, Santner SJ, Heitjan DF, Santen RJ (1995) Estrogen deprivation causes estradiol hypersensitivity in human breast cancer cells. *J Clin Endocrinol Metab* 80(10):2918–2925. doi:10.1210/jcem.80.10.7559875
- Miller WR, Larionov AA (2012) Understanding the mechanisms of aromatase inhibitor resistance. *Breast Cancer Res* 14(1):201. doi:10.1186/bcr2931
- Oesterreich S, Davidson NE (2013) The search for ESR1 mutations in breast cancer. *Nat Genet* 45(12):1415–1416. doi:10.1038/ng.2831
- Oesterreich S, Zhang P, Guler RL, Sun X, Curran EM, Welshons WV, Osborne CK, Lee AV (2001) Re-expression of estrogen receptor alpha in estrogen receptor alpha-negative MCF-7 cells restores

- both estrogen and insulin-like growth factor-mediated signaling and growth. *Cancer Res* 61(15):5771–5777
27. Pathiraja TN, Nayak SR, Xi Y, Jiang S, Garee JP, Edwards DP, Lee AV (2014) Epigenetic reprogramming of HOXC10 in endocrine-resistant breast cancer. *Sci Transl Med* 6(229):229ra241. doi:10.1126/scitranslmed.3008326
 28. Phuong NT, Kim SK, Lim SC, Kim HS, Kim TH, Lee KY, Ahn SG, Yoon JH, Kang KW (2011) Role of PTEN promoter methylation in tamoxifen-resistant breast cancer cells. *Breast Cancer Res Treat* 130(1):73–83. doi:10.1007/s10549-010-1304-2
 29. Rangasamy D (2010) Histone variant H2A.Z can serve as a new target for breast cancer therapy. *Curr Med Chem* 17(28):3155–3161
 30. Robinson DR, Wu YM, Vats P, Su F, Lonigro RJ, Cao X, Kalyana-Sundaram S et al (2013) Activating ESR1 mutations in hormone-resistant metastatic breast cancer. *Nat Genet* 45(12):1446–1451. doi:10.1038/ng.2823
 31. Santen RJ, Song RX, Masamura S, Yue W, Fan P, Sogon T, Hayashi S, Nakachi K, Eguchi H (2008) Adaptation to estradiol deprivation causes up-regulation of growth factor pathways and hypersensitivity to estradiol in breast cancer cells. *Adv Exp Med Biol* 630:19–34
 32. Santen RJ, Song RX, Zhang Z, Kumar R, Jeng MH, Masamura A, Lawrence J Jr, Berstein L, Yue W (2005) Long-term estradiol deprivation in breast cancer cells up-regulates growth factor signaling and enhances estrogen sensitivity. *Endocr Relat Cancer* 12(Suppl 1):S61–S73. doi:10.1677/erc.1.01018
 33. Santen R, Jeng MH, Wang JP, Song R, Masamura S, McPherson R, Santner S, Yue W, Shim WS (2001) Adaptive hypersensitivity to estradiol: potential mechanism for secondary hormonal responses in breast cancer patients. *J Steroid Biochem Mol Biol* 79(1–5):115–125
 34. Santoro, S W, and C. Dulac. (2012) The activity-dependent histone variant H2BE modulates the life span of olfactory neurons. *Elife* 1: e00070. doi:10.7554/eLife.00070
 35. Svtelias A, Gevry N, Grondin G, Gaudreau L (2010) H2A.Z over-expression promotes cellular proliferation of breast cancer cells. *Cell Cycle* 9(2):364–370
 36. Talbert PB, Henikoff S (2010) Histone variants—ancient wrap artists of the epigenome. *Nat Rev Mol Cell Biol* 11(4):264–275. doi:10.1038/nrm2861
 37. Tanaka M, Hennebold JD, Macfarlane J, Adashi EY (2001) A mammalian oocyte-specific linker histone gene H1oo: homology with the genes for the oocyte-specific cleavage stage histone (cs-H1) of sea urchin and the B4/H1M histone of the frog. *Development* 128(5):655–664
 38. Tomonaga T, Matsushita K, Yamaguchi S, Oohashi T, Shimada H, Ochiai T, Yoda K, Nomura F (2003) Overexpression and mistargeting of centromere protein-a in human primary colorectal cancer. *Cancer Res* 63(13):3511–3516
 39. Valdes-Mora F, Song JZ, Statham AL, Strbenac D, Robinson MD, Nair SS, Patterson KI, Tremethick DJ, Stirzaker C, Clark SJ (2012) Acetylation of H2A.Z is a key epigenetic modification associated with gene deregulation and epigenetic remodeling in cancer. *Genome Res* 22(2):307–321. doi:10.1101/gr.118919.110
 40. Vardabasso C, Hasson D, Ratnakumar K, Chung CY, Duarte LF, Bernstein E (2014) Histone variants: emerging players in cancer biology. *Cell Mol Life Sci* 71(3):379–404. doi:10.1007/s00018-013-1343-z
 41. Waggott D, Chu K, Yin S, Wouters BG, Liu FF, Boutros PC (2012) NanoStringNorm: an extensible R package for the pre-processing of NanoString mRNA and miRNA data. *Bioinformatics* 28(11):1546–1548. doi:10.1093/bioinformatics/bts188
 42. Yue W, Wang JP, Conaway M, Masamura S, Li Y, Santen RJ (2002) Activation of the MAPK pathway enhances sensitivity of MCF-7 breast cancer cells to the mitogenic effect of estradiol. *Endocrinology* 143(9):3221–3229. doi:10.1210/en.2002-220186